A Full-Wave Analysis Method for Open Microstrip Structures

TATSUO ITOH, SENIOR MEMBER, IEEE, AND WOLFGANG MENZEL

Abstract—**A method for analyzing characterisitcs of open microstrip disk structures is presented. The method is based on the spectral domain immittance matrix approach, and all the wave phenomena associated with the structures are incorporated. The method provides a number of unique and convenient features both in analytical and numerical phases. A numerical example illustrating the usefulness of the method is included. Some numerical results are compared with experimental data.**

I. INTRODUCTION

A NUMBER of theoretical analyses of printed circuit antenna structures appeared recently (for example; [1]). Many of these analyses are based on the quasi-static model of printed circuit structures. One typically computes the resonant frequency of the hypothetical closed resonator derived from the actual structure by placing a magnetic side wall extending from the microstrip to the ground plane. Magnetic current components computed from this resonator model are used to calculate the radiation patterns. The results so obtained indicate good agreement with experimental data, and hence the theory seems quite useful.

Independent of the efforts on antennas, microstrip, and other printed circuit structures have been used in microwave and millimeterwave integrated circuits. As the frequency of operation is increased, it has been realized, and now it is widely known, that the quasi-static analyses of microstrip circuit elements are not accurate enough, and a more rigorous full-wave analysis is required. For instance, as for the analysis of microstrip disk resonators, a number of improved theoretical analyses appeared in the past [2]–[4]. It has been reported that the results by the full-wave analysis agree extremely well with results measured at high frequencies [4].

This paper presents a full-wave analysis of the open printed circuit structures such as those encountered in microstrip antennas as an eigenvalue problem with complex eigenvalue (resonant frequency). Since all the wave phenomena are incorporated in the analysis, it is believed useful for microstrip type antenna applications at higher frequencies. The method is based on the spectral domain immittance matrix approach developed recently [5]. In the formulation process the directions parallel to the substrate surface are completely separted from the normal direction by the use of the equivalent network for spectral waves. As we will see shortly, the formulation process is so simple that it may be accomplished almost by inspection. The method is quite versatile and may be applied to almost any type of printed structures including coplanar, slot, and microstrip–slot resonators. Additionally, since we solve the problem for the Fourier transforms of unknown current distributions on the strip or aperture electric fields on the substrate, the far field radiation patterns may be simply extracted.

Manuscript received February 12, 1980; revised June 23, 1980. This work was supported in part by the U.S. Army Research Office under Grant DAAG29-78-G-0145.

T. Itoh is with the Department of Electrical Engineering, University of Texas, Austin, TX 78712.

W. Menzel is with the Hochfrequenztechnik, AEG-Telefunken, D-7900 Ulm, Germany.

II. FORMULATION OF THE PROBLEM

Although the method may be applied to other printed circuit structures, we will use the simple rectangular open microstrip disk in Fig. 1 for the formulation. The microstrip is located on the substrate of relative dielectric constant ϵ_r and thickness d. The standard spherical coordinate (r, θ, ϕ) is superimposed on the (x, y, z) system so that the radiation pattern is expressed in terms of θ and ϕ. θ is measured from the z axis, and ϕ is the angle measured in the xy plane from the x axis. The broadside of the antenna (y axis) is, therefore, given by $\theta = \phi = \pi/2$. The top surface of the substrate is taken to be $y = 0$. In conventional analysis we would derive coupled homogeneous integral equations for current distributions $J_x(x, z)$ and $J_z(x, z)$:

$$\iint [Z_{xx}(x-x', z-z')J_x(x', z') + Z_{xz}(x-x', z-z')J_z(x', z')]\, dx'\, dz' = 0 \tag{1}$$

$$\iint [Z_{zx}(x-x', z-z')J_x(x', z') + Z_{zz}(x-x', z-z')J_z(x', z')]\, dx'\, dz' = 0 \tag{2}$$

where the integrations are over the strip and the equations are valid for (x, z) on the strip. As is well-known, (1) and (2) state that E_x and E_z are zero on the strip. These equations can be solved for the complex resonant frequency and the current components J_x and J_z, provided all the dyadic Green's function components Z_{xx}, $Z_{xz} = Z_{zx}$, and Z_{zz} are available which are functions of the frequency. In the radiating structure, this resonant frequency becomes complex, and its imaginary part accounts for the energy loss due to radiation.

Instead of (1) and (2), we will introduce the spectral domain method. The domain of (1) and (2) is first extended to the infinite space and then Fourier transforms are taken. We obtain

$$\tilde{Z}_{xx}(\alpha, \beta)\tilde{J}_x(\alpha, \beta) + \tilde{Z}_{xz}(\alpha, \beta)\tilde{J}_z(\alpha, \beta) = \tilde{E}_x(\alpha, \beta, 0) \tag{3}$$

$$\tilde{Z}_{zx}(\alpha, \beta)\tilde{J}_x(\alpha, \beta) + \tilde{Z}_{zz}(\alpha, \beta)\tilde{J}_z(\alpha, \beta) = \tilde{E}_z(\alpha, \beta, 0) \tag{4}$$

where the Fourier transform is defined via

$$\tilde{\psi}(\alpha, \beta) = \int_{-\infty}^{\infty} \int_{-\infty}^{\infty} \psi(x, z) e^{j(\alpha x + \beta z)}\, dx\, dz. \tag{5}$$

0018-926X/81/0100-0063$00.75

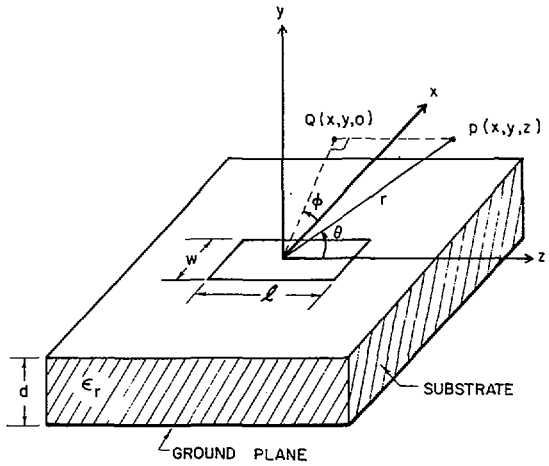

Fig. 1. Open microstrip resonant structure.

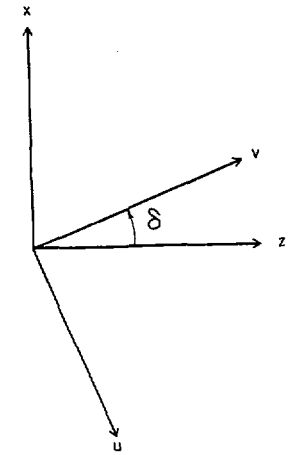

Fig. 2. Coordinate transformation.

Notice also that the right-hand sides of (3) and (4) are no longer zero because they are the Fourier transforms of E_x and E_z on the substrate surface which are obviously nonzero except on the strip. Although (3) and (4) contain four unknowns, $\tilde{J}_x$, $\tilde{J}_z$, $\tilde{E}_x$, and $\tilde{E}_z$, two of them, $\tilde{E}_x$ and $\tilde{E}_z$ may eliminated later in the solution process, and we can derive a homogeneous set of equations which can be solved for the complex resonant frequency.

The impedance coefficients $\tilde{Z}_{xx}$, $\tilde{Z}_{xz}$, and $\tilde{Z}_{zz}$ may be obtained by writing field distributions in the substrate and air region and applying the interface condition at the air-substrate surface. This process is straightforward. However, the application of the spectral domain immittance approach [5] is quite illustrative for such a process as described below. These coefficients are actually impedance matrix elements that relate $\tilde{J}_x$ and $\tilde{J}_z$ with $\tilde{E}_x$ and $\tilde{E}_z$. We will make use of equivalent transmission lines for the derivation. To this end, we first recognize that, from the definition of the inverse Fourier transform

$$\psi(x,z)=\frac{1}{(2\pi)^2}\int_{-\infty}^{\infty}\int_{-\infty}^{\infty}\tilde{\psi}(\alpha,\beta)e^{-j(\alpha x+\beta z)}\,d\alpha\,d\beta, \quad (6)$$

all the field components are superpositions over α and β of inhomogeneous (in y) waves propagating in the direction δ from the z axis where $\delta=\cos^{-1}(\beta/\xi)$, $\xi=\sqrt{\alpha^2+\beta^2}$. For each δ, the waves may be decomposed into TM to $y(\tilde{E}_y, \tilde{E}_v, \tilde{H}_u)$ and TE to $y(\tilde{H}_y, \tilde{E}_u, \tilde{H}_v)$ where the coordinates v and u are as shown in Fig. 2 and related with (x, z) via

$$u=z\sin\delta-x\cos\delta \quad (7)$$

$$v=z\cos\delta+x\sin\delta. \quad (8)$$

Next, we recognize that, if there were a current component $\tilde{J}_v$, it generates only the TM fields, and only the TE fields are generated by the $\tilde{J}_u$. Hence it is possible to draw equivalent circuits for the TM and TE fields as shown in Fig. 3. The wave admittances in each region are

$$Y_{\mathrm{TM}i}=\frac{\tilde{H}_u}{\tilde{E}_v}=\frac{j\omega\epsilon_0\epsilon_i}{\gamma_i}, \qquad i=1,2 \quad (9)$$

$$Y_{\mathrm{TE}i}=-\frac{\tilde{H}_v}{\tilde{E}_u}=\frac{\gamma_i}{j\omega\mu}, \qquad i=1,2 \quad (10)$$

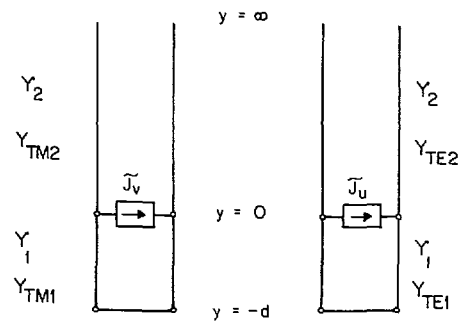

Fig. 3. Spectral domain equivalent circuits.

where $\gamma_i^2=\alpha^2+\beta^2-\epsilon_i k^2$ is the propagation constant in the y direction in the ith region. Also $\epsilon_1=\epsilon_r$ and $\epsilon_2=1$. γ_i is real for decaying wave and is imaginary for wave propagaing in the y direction. All the boundary conditions which these TE and TM waves are required to satisfy are incorpated in the equivalent circuits. Specifically, the electric conductor boundary at $y=-d$ is represented by the short circuit conditions in the equivalent circuits, whereas the radiation condition at $y\to\infty$ corresponds to infinitely long transmission lines for $y>0$. The continuity condition of tangential electric fields at $y=0$ can be seen from the fact that the voltages on both sides of the junction $y=0$ are equal, while the discontinuity of the magnetic field on both sides of the strip is represented by the equivalent current sources J_v and J_u for the spectral wave. In these equivalent circuits, the voltages, E_v and E_u at $y=0$ are related to the current sources via

$$\tilde{E}_v(\alpha,\beta,0)=\tilde{Z}_0{}^e(\alpha,\beta)\tilde{J}_v(\alpha,\beta) \quad (11)$$

$$\tilde{E}_u(\alpha,\beta,0)=\tilde{Z}_0{}^h(\alpha,\beta)\tilde{J}_u(\alpha,\beta). \quad (12)$$

It is easy to see that $Z_0{}^e$ and $Z_0{}^h$ are input impedances looking into the equivalent circuits at $y=0$ and hence are expressed as

$$\tilde{Z}_0{}^e=\frac{1}{Y_+{}^e+Y_-{}^e} \quad (13)$$

$$\tilde{Z}_0{}^h=\frac{1}{Y_+{}^h+Y_-{}^h} \quad (14)$$

where $Y_+{}^e$ and $Y_-{}^e$ are input admittances looking down and

up at $y = 0$ in the TM equivalent circuit, and Y_+^h and Y_-^h are corresponding quantities in the TE circuit:

$$Y_+^e = Y_{TM1} \coth \gamma_1 d \qquad Y_-^e = Y_{TM2} \tag{15}$$

$$Y_+^h = Y_{TE1} \coth \gamma_1 d \qquad Y_-^h = Y_{TE2}. \tag{16}$$

The final step of the formulation consists of the mapping from the u, v cordiante for spectral waves corresponding to each δ. Because of the coordinate transform relations (7) and (8), $\tilde{E}_x$ and $\tilde{E}_z$ are linearly related to $\tilde{E}_u$ and $\tilde{E}_v$. Similarly, $\tilde{J}_x$ and $\tilde{J}_z$ are superposition of $\tilde{J}_u$ and $\tilde{J}_v$. When these relations are used, the impedance matrix elements in (3) and (4) are given by

$$\tilde{Z}_{xx}(\alpha, \beta) = N_x^2 \tilde{Z}_0^e + N_z^2 \tilde{Z}_0^h \tag{17}$$

$$\tilde{Z}_{xz}(\alpha, \beta) = N_x N_z(-\tilde{Z}_0^e + \tilde{Z}_0^h) \tag{18}$$

$$\tilde{Z}_{zz}(\alpha, \beta) = N_z^2 \tilde{Z}_0^e + N_x^2 \tilde{Z}_0^h \tag{19}$$

where N_x and N_z are transforming ratios given by

$$N_x = \frac{\alpha}{\sqrt{\alpha^2 + \beta^2}} = \sin \delta, N_z = \frac{\beta}{\sqrt{\alpha^2 + \beta^2}} = \cos \delta. \tag{20}$$

Notice that $\tilde{Z}_0^e$ and $\tilde{Z}_0^h$ are functions of $\alpha^2 + \beta^2$, and the ratio of α to β enters only through N_x and N_z.

III. DERIVATION OF THE EIGENVALUE EQUATION

We now have two ways to solve the original open microstrip problem. The conventional one is to use the integral equations (1) and (2) in the spectral impedance matrix elements given in (17)–(19). Another approach is the direct use of algebraic equations (3) and (4) as all the necessary quantities have been derived in the previous section. As discussed earlier, (3) and (4) contain four unknowns. Two of them, $\tilde{E}_x$ and $\tilde{E}_z$, however, are eliminated in the solution process based on the Galerkin's method. To this end, the unknown spectral current components $\tilde{J}_x$ and $\tilde{J}_z$ are expanded in terms of linear combinations of known basis functions

$$\tilde{J}_x(\alpha, \beta) = \sum_{m=1}^{M} c_m \tilde{J}_{xm}(\alpha, \beta) \tag{21}$$

$$\tilde{J}_z(\alpha, \beta) = \sum_{n=1}^{N} d_n \tilde{J}_{zn}(\alpha, \beta). \tag{22}$$

In selecting basis functions, we ensure that they are Fourier transforms of functions with finite support. That is, $\tilde{J}_{xm}$ and $\tilde{J}_{zn}$ are Fourier transforms of $J_{xm}(x, z)$ and $J_{zn}(x, z)$ which are nonzero only on the strip. Let us now substitue (21) and (22) into (3) and (4) and take the inner products of the resulting equations with each of basis function as the standard Galerkin's procedure calls for. The result is the following homogeneous matrix equation

$$\sum_{m=1}^{M} K_{pm}^{xx} c_m + \sum_{n=1}^{N} K_{pn}^{xz} d_n = 0, \quad p = 1, 2, \cdots, M$$

$$\sum_{m=1}^{M} K_{qm}^{zx} c_m + \sum_{n=1}^{N} K_{qn}^{zz} d_n = 0, \quad q = 1, 2, \cdots, N \tag{23}$$

where the typical matrix element is given by

$$K_{pn}^{xz} = \int_{-\infty}^{\infty} \int_{-\infty}^{\infty} \tilde{J}_{xp}(\alpha, \beta) \tilde{Z}_{xz}(\alpha, \beta) \tilde{J}_{zn}(\alpha, \beta)\, d\alpha\, d\beta. \tag{24}$$

Since K_{pn}^{xz}, etc., are functions of a frequency, a nontrivial solution of (23) is derived by seeking a complex frequency that makes the determinant of the coefficient matrix of (23) zero. The corresponding eigenvector (c_m, d_n) specifies the current distributions on the strip.

Notice that the right-hand side of (23) is zero. This is explained by writing a more specific process in the Galerkin's procedure. When a basis function is multiplied with (3) or (4), we typically have

$$\int_{-\infty}^{\infty} \int_{-\infty}^{\infty} \tilde{J}_{xp}(\alpha, \beta) \tilde{E}_x(\alpha, \beta, 0)\, d\alpha\, d\beta$$

$$= (2\pi)^2 \int_{-\infty}^{\infty} \int_{-\infty}^{\infty} J_{xp}(x, z) E_x(x, z, 0)\, dx\, dz \tag{25}$$

by virtue of the Parseval's relation. The right-hand side vanishes because J_x and E_x are nonzero only over regions of (x, z) complementary to each other, that is, J_x is zero outside the strip and E_x is zero on the strip.

Equation (23) is exact if $M = N \to \infty$. However, in practice, M and N must be finite, and such truncation introduces an approximation. If individual basis functions $\tilde{J}_{xm}$ and $\tilde{J}_{zn}$ are chosen such that their inverse Fourier transforms include qualitative natures of the true unknown current distributions, it is possible to use only a few basis functions to obtain good results, and the computation time can be reduced. Another important feature for time saving is to choose the basis functions which are expressed in closed forms. Although this is not always possible with strips that have general shapes, in the present rectangular strip one may use $J_{xm}(x, z)$ and $J_{zn}(x, z)$ which reasonably represent qualitative natures of the true components and still whose Fourier transforms are analytically obtainable. Choice of the basis functions have been studied in a number of recent publications [6], [7]. One possible choice for J_{xm} and J_{zm} is

$$J_{zm}(x, z) = \frac{\cos\left[(r-1)\pi \dfrac{2x}{w}\right]}{\sqrt{\left(\dfrac{w}{2}\right)^2 - x^2}} \frac{\cos\left[(2s-1)\pi \dfrac{z}{l}\right]}{\sqrt{\left(\dfrac{l}{2}\right)^2 - z^2}} \tag{26}$$

$$J_{xm}(x, z) = \frac{\sin\left[2r\pi \dfrac{x}{w}\right]}{\sqrt{\left(\dfrac{w}{2}\right)^2 - x^2}} \frac{\sin\left[(2s-1)\pi \dfrac{z}{l}\right]}{\sqrt{\left(\dfrac{l}{2}\right)^2 - z^2}} \tag{27}$$

where $r = 1, 2, \cdots$ and $s = 1, 2, \cdots$. Any combination of r and s provides a specific basis function. Therefore, the index m for the basis function is given by a combination of r and s. For instance, we can choose $m = 1$ for $r = s = 1$. The Fourier transforms of (26) and (27) are readily available as combina-

tions of the Bessel function of order zero. Notice also that the correct singularities of the current distribution at the edges are incorporated in (26) and (27). The current becomes singular of order $1/\sqrt{R}$ at the edges parallel to the current and zero of $\sqrt{R}$ at the edges normal to it, where R is the distance from the edge.

IV. FEATURES OF THE METHOD

The present method incorporates a number of unique features. Let us describe numerical aspects first and then go to more important analytical aspects. It has been proven in a number of papers on microstrip and other printed line structures that the spectral domain method is numerically quite efficient [4], [5]. For instance, accurate solutions are obtained by using a relatively small size matrix (23) such as $M = N = 1$ or 2. In contrast in many space domain analyses which typically deal with the coupled integral equations (1) and (2), the size of the matrix to be inverted is quite large if, for instance, the point matching is used. On the other hand, if Galerkin type procedures are used in the space domain, it is necessary first to perform the inverse Fourier transforms, which are extremely time consuming, to get the Green's functions and then to carry out the convolution integrals.

The time saving feature of the spectral domain method is caused essentially by two elements. First, it is possible to use basis functions which incorporate certain qualitative natures of the true current distributions such as the edge condition. This eliminates use of a large number of basis functions to accurately represent unknown current distributions. Second, in the spectral domain approach, we deal with algebraic rather than integral equations. It is not necessary to carry out the convolution integrals, and the spectral domain impedance functions are given in closed forms. Of course, the price we have to pay for such features is that the inner products to compute matrix elements ${K_{pm}}^{xx}$, etc., are infinite integrals. However, the integrands of these integrals decay as fast as α^{-2} and β^{-2} when the basis functions like those obtained from (26) and (27) are used, and hence the inner products can be computed without much difficulty. Nevertheless, the number of iterations for seeking a root should be minimized. Often, this can be as small as five to ten when a good subroutine is used. Besides, since the basis functions are not functions of the frequency, they need to be evaluated only once, contributing to the reduction of computation time.

Let us now turn our attention to more analytical features of the method. We go back to (17)–(19) and study their construction. We recognize that ${\tilde{Z}_0}^e$ and ${\tilde{Z}_0}^h$ are obtained from the equivalent circuits which extend in the y direction. The information in the x and z direction come in $\tilde{Z}_{xx}$, $\tilde{Z}_{xz}$, and $\tilde{Z}_{zz}$ only through the transforming ratios N_x and N_z. Also the information on the microstrip is contained only in the basis functions. This is not special at all because Z_{xx}, etc., are the Fourier transform of the Green's functions which are independent of the source shapes and related only to the location and the direction of the source.

When the resonances in the y-direction occur, the denominator of ${\tilde{Z}_0}^e$ or ${\tilde{Z}_0}^h$ becomes zero as a surface wave pole is encountered. The radiation phenomena are associated with the imaginary part of γ_2. Therefore, the visible region ($\alpha^2 + \beta^2 < k^2$) of the $\alpha\beta$ plane is responsible for radiation, and the surface wave poles occur on circles with radius $\sqrt{\alpha^2 + \beta^2}$ between $\sqrt{\epsilon_2}k$ and $\sqrt{\epsilon_1}k$. The invisible region $\alpha^2 + \beta^2 > k^2$ is responsible for the stored energy in the near region. The equivalent circuits do not, however, tell any directional information in the xz plane. Such is provided by the weighting functions $\tilde{J}_x$ and $\tilde{J}_z$.

What is presented in the previous paragraph is rather well-known. In the present eigenvalue problem, it is necessary to consider complex k's because only the complex frequency $\omega_c = \omega_r + j\omega_i$ can satisfy the system which loses energy by radiation. In the computation, we keep α and β to be real. Therefore, surface wave poles are not crossed. However, since they are located near the integration surface, their effects are contained in the formulation.

Once the problem is solved, far field radiation patterns are given from $\tilde{E}_x$ and $\tilde{E}_z$ as they are Fourier transforms of the electric field:

$$E_\theta(\phi, 0) \propto \sin\phi \tilde{E}_z(\alpha, \beta)$$

$$E_\phi(\phi, \theta) \propto \cos\phi \cos\theta \tilde{E}_z(\alpha, \beta) + \sin\phi \tilde{E}_x(\alpha, \beta) \tag{28}$$

with

$$\alpha = k \sin\theta \cos\phi$$

$$\beta = k \cos\theta \tag{29}$$

and $\tilde{E}_x$, $\tilde{E}_z$ given by (3), (4), and (21), (22). In the E-plane ($\theta = \pi/2$)

$$E_\theta \propto \sum_n d_n \tilde{Z}_{zz}(0, k\cos\theta)\tilde{J}_{an}(0, k\cos\theta) \tag{30}$$

and in the H-plane ($\theta = \pi/2$)

$$E_\theta \propto \sin\phi \sum_n d_n \tilde{Z}_{zz}(k\cos\phi, 0)\tilde{J}_{zn}(k\cos\phi, 0). \tag{31}$$

V. NUMERICAL RESULTS

A Fortran program has been made to perform the calculations described above. The integration over the $\alpha - \beta$ plane has to be done numerically. As $\tilde{J}_z \propto 1/\sqrt{\alpha\beta^3}$ and $\tilde{Z}_{zz} \propto \beta^2/\sqrt{\alpha^2 + \beta^2}$ for large agreements α and β (and similar relations are valid for J_x, $\tilde{Z}_{xx}$, and $\tilde{Z}_{xz}$), the integration converges with $1/(\alpha\beta\sqrt{\alpha^2 + \beta^2})$.

Numerical and experimental evaluations have been done with RT-Duriod substrates with $\epsilon_r = 2.35$ and a thickness of $d = 1.58$ mm. Table I summarizes computed resonant frequencies for two different microstrip sizes. For a narrow element ($l = 1$ cm, $w = 0.2$ cm), the real part of the computed resonant frequency does not change much by using different number of basis functions. The imaginary part indicating the energy lost by radiation is extremely small.

Experiments have been performed for the patch antenna made of a microstrip of $l = 1$ cm and $w = 1.5$ cm. First, the antenna element was fed by a 100-Ω microstrip line connected directly (or inductively) to the element. The measured resonant frequency (f_r) was 8.75 GHz. Next, we created a gap between the antenna element and the feed line to get a weak capacitive coupling. The measured resonant frequency then was 8.29 GHz which results in a differenc of 1.4 percent, compared with the theoretical value obtained by using two $\tilde{J}_{zm}$ and one $\tilde{J}_{xm}$, that is, 8.41 GHz. This can be due to the uncertainty of ϵ_r (±2 percent) or the substrate thickness d. In any case, it is felt that more basis functions have to be taken into account for this very wide element.

The bandwidth of the capacitively coupled element was 0.6

TABLE I
CALCULATED RESONANT FREQUENCY

Structure ℓ(cm)	w(cm)	No. of basis functions J_z	J_x	Resonant frequency (GHz)
1	0.2	1	0	$9.616 + j\ 0.171 \times 10^{-9}$
		1	1	$9.608 + j\ 0.128 \times 10^{-6}$
		1	0	8.586 + j 0.28
1	1.5	1	1	8.05 + j 0.21
		2*	1	8.41 + j 0.272

$\epsilon_r = 2.35$, d = 1.58 mm

* with different x-dependences

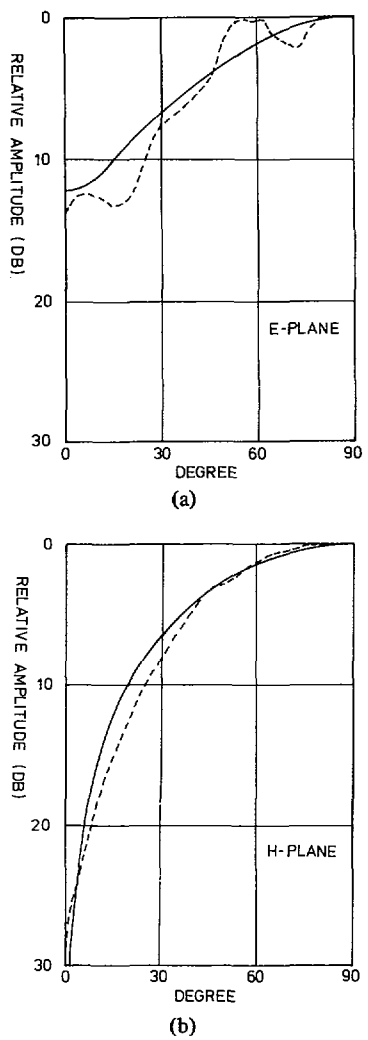

Fig. 4. Radiation patterns. — theory, ---- measured. (a) *E*-Plane. (b) *H*-plane.

GHz in the experiment compared with the theoretical one of 0.54 GHz. The latter was derived from the definition of Q:

$$Q = \frac{\omega_r}{2\omega_i}. \tag{32}$$

The difference between the resonant frequencies in the inductive and capacitive coupling cases seems to be due mainly to the relatively high inductance of the impedance step when the element is coupled directly to the feed line. This shows the necessity of getting more information on the discontinuity effects involved in microstrip antenna circuits.

The radiation patterns in the *E*- and *H*-planes were measured with the capacitively coupled element at 8.29 GHz. Fig. 4 shows the measured and computed (with two $\tilde{J}_{zm}$ and one $\tilde{J}_{zm}$) patterns. The experimental *E*-plane pattern contains large ripples caused by the small substrate size and radiation from the feed.

VI. CONCLUSION

We have presented a full-wave method for analyzing open printed circuit structures. The formulation is based on the spectral domain immittance matrix derived from the spectral domain equivalent circuits. In the solution process, Galerkin's method is used. The method contains several attractive features from both analytical and numerical points of view. Although a microstrip structure is treated in the paper, the method itself is quite general and is applicable to other types of printed structures such as the coplanar and slot lines. Also, it is quite straightforward to extend the method to structures involving stratified substrates, several radiating elements, and even those containing conductor elements at different interfaces of stratified substrate [5]. It will be constructive to test the present method with simpler basis functions. Such studies may be useful for more complicated strip structures for which less sophisticated basis functions need to be used.

ACKNOWLEDGMENT

The authors thank Dr. B. Rembold of AEG-Telefunken, for his giving them the opportunity to complete the present work.

REFERENCES

[1] J. R. James and G. J. Wilson, "Microstrip antennas and arrays. Pt. 1—Fundamental action and limitations," *IEE J. Microwaves, Opt., Acoust.*, vol. 1, pp. 157–164, Sept. 1977.

[2] T. Itoh and R. Mittra, "Analysis of a microstrip disk resonator," *Arch. Elek. Ubertragung.*, vol. 27, pp. 456–458, Nov. 1973.

[3] I. Wolff and N. Knoppik, "Rectangular and circular microstrip disk capacitors and resonators," *IEEE Trans. Microwave Theory Tech.*, vol. MTT-22, pp. 857–864, Oct. 1974.

[4] T. Itoh, "Analysis of microstrip resonators," *IEEE Trans. Microwave Theory Tech.*, vol. MTT-22, pp. 946–952, Nov. 1974.

[5] ——, "Spectral domain immittance approach for dispersion characteristics of shielded microstrips with tuning septums," presented at the 9th European Microwave Conf., Brighton, England, Sept. 17–21, 1979.

[6] R. H. Jansen, "High-speed computation of single and coupled microstrip parameters including dispersion, high-order modes, loss and finite strip thickness," *IEEE Trans. Microwave Theory Tech.*, vol. MTT-26, pp. 75–82, Feb. 1978.

[7] E. F. Kuester and D. C. Chang, "An appraisal of methods for computation of the dispersion characteristics of open-microstrip," *IEEE Trans. Microwave Theory Tech.*, vol. MTT-27, pp. 691–694, July 1979.

Tatsuo Itoh (S'69–M'69–SM'74) received the Ph.D. degree in electrical engineering from the University of Illinois, Urbana, in 1969.

From September 1966 to April 1976 he was with the Electrical Engineering Department, University of Illinois. From April 1976 to August 1977 he was a Senior Research Engineer in the Radio Physics Laboratory, SRI International, Menlo Park, CA. From August 1977 to June 1978 he was an Associate Professor at the University of Kentucky, Lexington. In July 1978 he joined the faculty at The University of Texas at Austin, where he is now an Associate Professor of Electrical Engineering and Director of the Microwave Laboratory. During the summer 1979, he was a Guest Researcher at AEG-Telefunken, Ulm, West Germany.

Dr. Itoh is a member of the Institute of Electronics and Communication Engineers of Japan, Sigma Xi, and Commissions B and C of USNC/URSI. He is a Registered Professional Engineer in the State of Texas.

Wolfgang Menzel was born in Brilon-Wald, West Germany, on December 10, 1948. He received the Dipl. Ing. degree from the Technical University of Aachen, Germany, in 1974, and the Dr. Ing. degree from the University of Duisburg, Germany, in 1977.

From 1974–1979, he was working at the University of Duisburg on microstrip circuit problems. Since 1979, he has joined AEG-Telefunken in Ulm, Germany, working on integrated millimeter-wave components and planar antennas.

Analysis of a Circular Microstrip Disk Antenna with a Thick Dielectric Substrate

WENG CHO CHEW AND JIN AU KONG, SENIOR MEMBER, IEEE

Abstract—**The problem of a circular microstrip disk excited by a probe is solved using rigorous analysis. The disk is assumed to have zero thickness, and the current on the probe is taken to be uniform. Using vector Hankel transforms the problem is formulated in terms of vector dual-integral equations, from which the unknown current can be solved for. Due to the singular nature of the current distribution arising from probe excitation, the direct application of Galerkin's basis function expansion method gives a slowly convergent result. Therefore the singular part of the current is removed since the singularity is known *a priori*. The unknown current to be solved for is then regular and tenable to Galerkin's method of analysis. It is shown that this analysis agrees with the single-mode approximation when the dielectric substrate layer is thin, and that it deviates from the single-mode approximation when the substrate layer is thick. Excellent agreement of both the computed real and imaginary parts of the input impedance with experimental data is noted. The radiation patterns and the current distributions on the disk are also presented.**

I. INTRODUCTION

THE RECENT advent of the microstrip antenna has aroused interest in both the experimental and theoretical analysis of the antenna [1]–[8]. Due to the inherent narrow bandwidth of the microstrip antenna, it is desirable to find methods to increase the bandwidth. It is well-known that, by increasing the thickness of the dielectric substrate, the bandwidth of the antenna can be increased [7], [8]. From a theoretical point of view it is important to analyze both thin- and thick-substrate microstrip antennas and to investigate their respective regions of validity in theory and applicability. Existing techniques for calculating the input impedance of microstrip disk antennas are only valid for thin dielectric substrates [2], [4], [8]. This is partly due to the use of the free-space Green's function in calculating the radiation loss and thus neglecting the dielectric effects [2], [4], and partly to the perturbative arguments employed [8]. In the perturbative approach the microstrip disk antenna is thought of as a perturbation of a magnetic wall cavity, implying its high-Q factor. The high-Q factor allows the approximation of the field inside the microstrip antenna with a single mode.

In this paper we shall present a method to calculate the input impedance of a circular microstrip disk under a probe excitation which is viable beyond the range of validity of the single-mode approximation in [8]. We shall make use of vector Hankel transforms (VHT's) in our formulation. The VHT is devised by the authors in [7] where its associated properties are also derived. It is found that the use of VHT's simplifies the otherwise complicated analysis.

II. FORMULATION

We wish to obtain the field solution of a circular printed-circuit antenna under a probe excitation. To do this we first have to obtain the field in the upper half-space due to a finite-radius vertical probe embedded in the first layer of a stratified half-space as shown in Fig. 1.

Using the dyadic Green's function formalism we can show that the $\hat{z}$ component of the electric field, due to a vertical probe of length L and radius R with uniform current I in an

Manuscript received May 1, 1980; revised August 10, 1980. This work was supported by Schlumberger-Doll Research Center and the Joint Services Electronics Program under Contract DAAG-29-78-C-0020.

The authors are with the Research Laboratory of Electronics, Department of Electrical Engineering and Computer Science, Massachusetts Institute of Technology, Cambridge, MA 02139.

0018-926X/81/0100-0068$00.75